Supplementary Information (SI) for Nanoscale.
This journal is © The Royal Society of Chemistry 2024

Supporting Information for

Amplification-Free Detection of Mycobacterium Tuberculosis Using CRISPR-Cas12a and Graphene Field-Effect Transistors

Weiqi Wang[a,b,‡], Huanyu Du,[a,b,‡] Changhao Dai,[a,b] Hongwenjie Ma,[a,b] Shi Luo,[a,b] Xuejun Wang,[a,b] Mingquan Guo,[c,*] Derong Kong,[a,b,*] Dacheng Wei[a,b,*]

[a] State Key Laboratory of Molecular Engineering of Polymers, Department of Macromolecular Science, Fudan University, Shanghai 200433, China

[b] Institute of Molecular Materials and Devices, Fudan University, Shanghai 200433, China

[c] Department of Laboratory Medicine, Shanghai Public Health Clinical Center, Fudan University, Shanghai 201508, China

[‡] The authors contributed equally to this paper

*Corresponding email: weidc@fudan.edu.cn; drkong@fudan.edu.cn; gmqjiandan@163.com

Section S1. Experimental details

Fabrication of the graphene field-effect transistors

A clean SiO_2/Si substrate with a silicon thickness of 500 μm and an oxidation insulation layer thickness of 500 nm is utilized. The sacrificial layer LOR 3A and the photoresist S1813 are applied to the substrate surface using two spin coating methods. Subsequently, the sample is exposed in the lithography machine Microwriter ML3 to obtain the FET source leakage electrode pattern. On the lithographic SiO_2/Si substrate, a deposition of 5 nm chromium (Cr) followed by 38 nm gold (Au) is performed using an Angstrom Engineering thermal evaporator. Chromium is incorporated to enhance the adhesion and contact between the gold electrode and SiO_2/Si substrate. Excess metal and photoresist are removed by immersing it into Remover PG solution, leaving only the gold electrode at the source leakage electrode pattern. Monolayer graphene is synthesized on a copper foil (25 μL) through chemical vapor deposition in a tube furnace (GSL 1200X-S). PMMA powder with a molecular weight of 996k is dissolved in either anisole, forming an 8 wt % PMMA solution which acts as a support when spun onto a single layer of graphene. The graphene undergoes acid etching for transfer onto a silicon substrate, followed by electrode placement and removal of surface PMMA using acetone. Finally, standard lithography combined with O_2 plasma etching (ZEPTO RIE) defines the size of sensing channel (W × L:100×30 μm^2). Any remaining photoresist is eliminated through rinsing with acetone and developer solution.

Cas12a modification

After the transfer and patterning of graphene, the device is immersed in a 5 mmol PASE solution overnight. It is then washed with ethanol and water before placing the PDMS tank above the sensor channel. The crRNA sequence is purchased from Bioligo Biotechnology and sequenced. AacCas12a (purchased from the company) is stored at −20 ℃. Cas12a protein is diluted to a concentration of 5 nM using 1 × NE Buffer, while crRNA is diluted to a concentration of 2 nM using TE Buffer. Cas12a (5 nM, 35 μL) and crRNA (2 nM, 50 μL) are mixed and incubated at 37 °C for 30 minutes in the PCR (Polymerase Chain Reaction) thermal cycler. After complete binding between Cas12a and crRNA, the mixture is added to the PDMS well and kept at room temperature for at least 4 hours to allow fixation of the Cas12a-crRNA ribonucleoprotein (RNP) complex on the graphene surface.

Clinical Samples

Serum samples are collected from 30 patients with TB or latent TB and 26 healthy people from Shanghai Public Health Clinical Center. The MagMAX^{TM} DNA Multi-Copy Ultra 2.0 kit (Thermo Fisher) is used to achieve high throughput separation of DNA from serum. The specific operation process is as follows. After adding protease k to the serum sample, it is heated at 65 ℃ for 20 minutes to destroy the bacterial structure and release the nucleic acid DNA. The DNA Binding Bead Mix consists of a binding solution and DNA binding beads, which are introduced into treated serum samples for the purpose of adsorbing the DNA released through cleavage. Shake the mixture at a speed of 800 revolutions per minute (rpm) for 5 minutes, allow it to settle and employ magnets to facilitate the precipitation of magnetic beads, followed by draining the supernatant liquid. The magnetic beads are subsequently subjected to multiple rinses with a cleaning solution, followed by the elution of DNA from the beads and its subsequent storage in the DNA eluent. The study is given ethical approval by the Ethics Committee of Shanghai Public Health Clinical Center (Approval ID: #2021−S057−03).

Preparation of DNA sequence sample

Escherichia coli specific sequence sipDNA, Streptococcus unperturbans specific sequence 16sDNA and Is1081 are purchased from Bioligo Biotechnology and sequenced. The powdered sample is centrifuged at 4 ℃ (4000 rpm, 5 min), and then TE buffer is added until reaching the storage concentration. Before the test, TE Buffer was used to dilute the samples, and Thermo Scientific NanoDrop One/OneC spectrophotometer is used to detect and verify the DNA concentration in the target samples. In the specific validation experiments, the concentration of Is1081 is 6×10^{-16} M, and the concentration of sipDNA and 16sDNA is 6×10^{-15} M. All samples are stored in a −20 ℃ refrigerator and the tests are carried out at room temperature.

Section S2. Calculation

Calculation of limit of detection（LoD）

As previously reported, $|\Delta V_{\text{Dirac}}|$ values are shown to be linearly correlated with the concentration of analyte. In our work, linear regression curves are plotted using the $|\Delta V_{\text{Dirac}}|$ values for samples with at least 5 concentration gradients. The measurements are repeated 3 times at each concentration. The LoD is read based on the noise level and the intercepted value of the linear standard curve. The noise level is taken to be three times the maximum signal response of the blank control test. In Fig. 2B, this equation is linear fitted as:

$$|\Delta V_{Dirac}| = 2.445 \ln C_{target} + 52.46 \quad (1)$$

C_{target} represents the concentration of analyte, Is1018 in this case. With the average background of the device $|\Delta V_{\text{Dirac}}|$ signal is 3.13 mV, the cutoff value for LoD calculation is 9.39 mV. Thus, in equation (1), C_{target} is 2.42×10^{-18} mol L^{-1}.

Section S3. Supplementary Figures

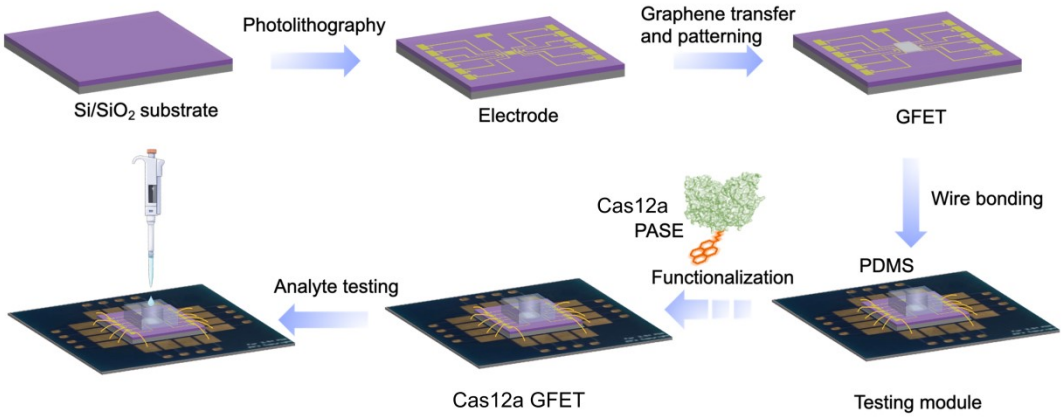

Figure S1. Workflow diagram for preparing and using a Cas12a-FET biosensor. The process includes photolithography, electrode fabrication, graphene transfer and patterning, Cas12a functionalization, wire bonding and analyte testing. The electrode pattern is created on the silicon wafer by photolithography, after which the chromium-gold electrodes are deposited onto Si/SiO_2 substrate using a thermal vapor deposition process. Then the photoresist and excess metal on the surface of the wafer are removed by a solvent method. Monolayer graphene is transfered as the conductive channel, on which Cas12a probes are immobilized through covalent bonding with PASE in a PDMS well, after the substrate is bonded to a printed circuit board. Clinical sample is added to the testing module and a signal can be detected in minutes.

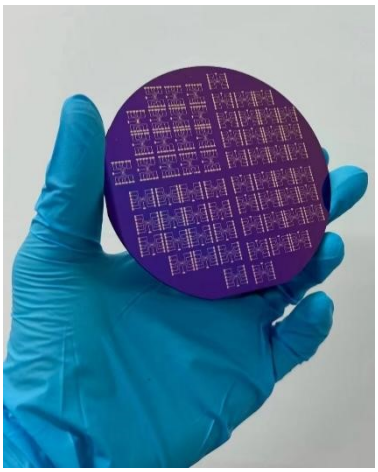

Figure S2. Photograph of fabricated FET device array on a 4−inch wafer.

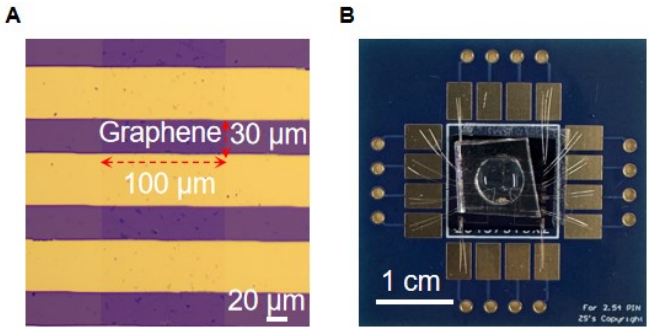

Figure S3. (A) Optical micrograph of the sensor. The scale bar is 20 µm. (B) Photograph of the packaged device. The scale bar is 1 cm.

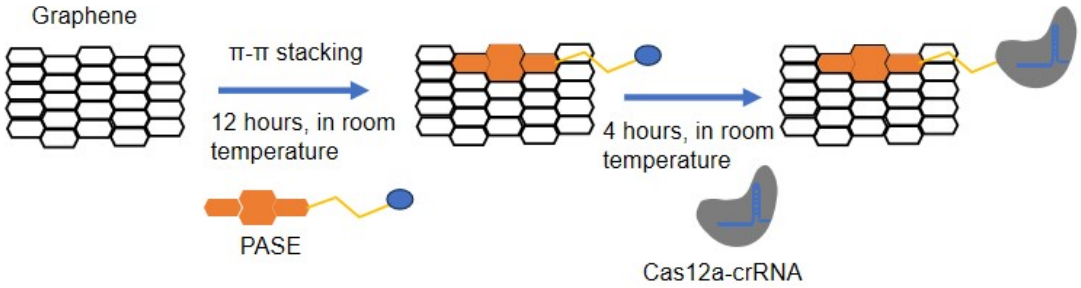

Figure S4. Modification of probes on the graphene with PASE. After immersing the GFET device in acetone solution of 5 mM PASE for 12 hours, the pyrene group in 1−pyrenebutyric acid N-hydroxysuccinimide ester can be effectively combined with graphene through π–π stacking. The Cas12b-crRNA was covalently immobilized onto the graphene surface in 1×NE buffer for 4 hours, via ester group cross-linking with amino groups present in proteins.

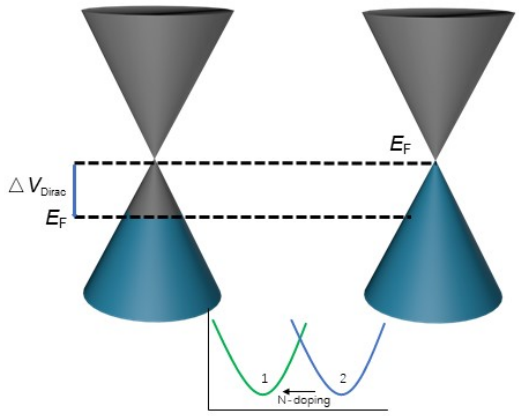

Figure S5. Effect of the Fermi energy level change on GFET transfer curve. When the charged analyte is close to or directly in contact with graphene, an induced charge will appear under electric field induction, which will cause the doping of graphene and affect the carrier concentration in it, resulting in a left shift in the transfer curve.

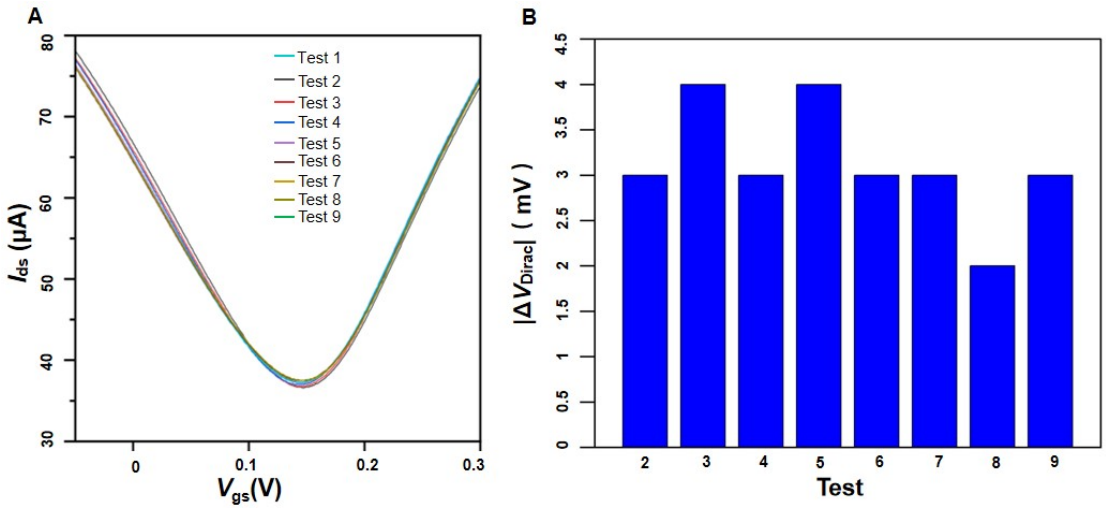

Figure S6. The background noise of the GFET biosensor. (A) I_{ds}−V_{gs} curves of a Cas12a-GFET in addition of 1×NE buffer for 9 times. (B) $|\Delta V_{Dirac}|$ response values of the Cas12a-GFET in the tests. $|\Delta V_{Dirac}|=|V_{test}-V_0|$, where V_0 is the V_{Dirac} in test 1; V_{test} is the V_{Dirac} in tests 2−9. The average offset of the Dirac point is 3.13 mV.

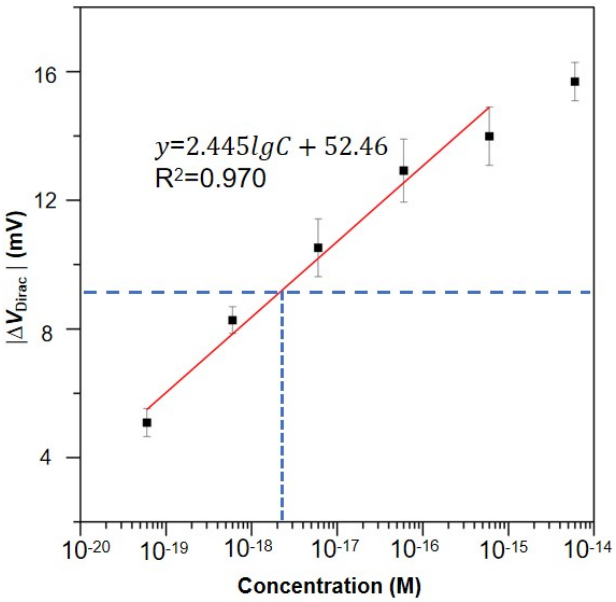

Figure S7. $|\Delta V_{\mathrm{Dirac}}|$ of Cas12a−GFETs upon the addition of Is1081 at concentrations from 6×10^{-20} to 6×10^{-15} M in 1×NE buffer. With the average background of the device $|\Delta V_{\mathrm{Dirac}}|$ signal being ~3.13 mV, the cutoff value is ~9.39 mV. The linear regression equation is calculated as $|\Delta V_{Dirac}| = 2.445\lg C_{target} + 52.46$, and the LoD is calculated to be 2.42×10^{-18} M. Error bars are determined by the standard deviation from 3 devices.

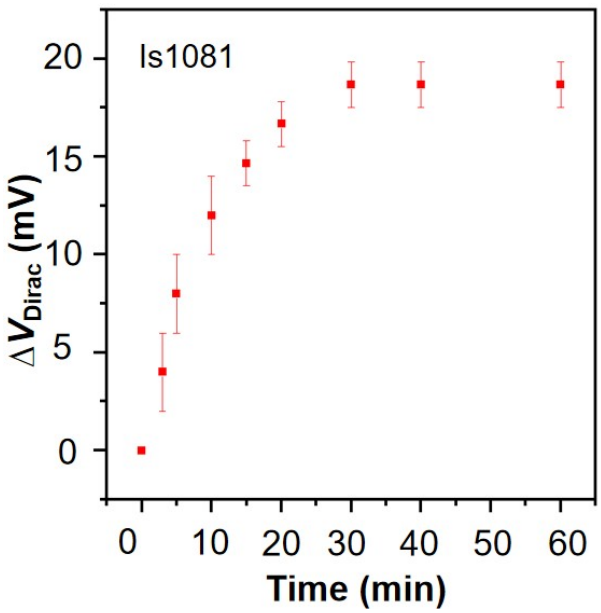

Fig. S8 $|\Delta V_{Dirac}|$ of Cas12a−GFETs measured at different times after the addition of Is1081 at concentrations of 6×10^{-16} M. Error bars are determined by the standard deviation from 3 devices.

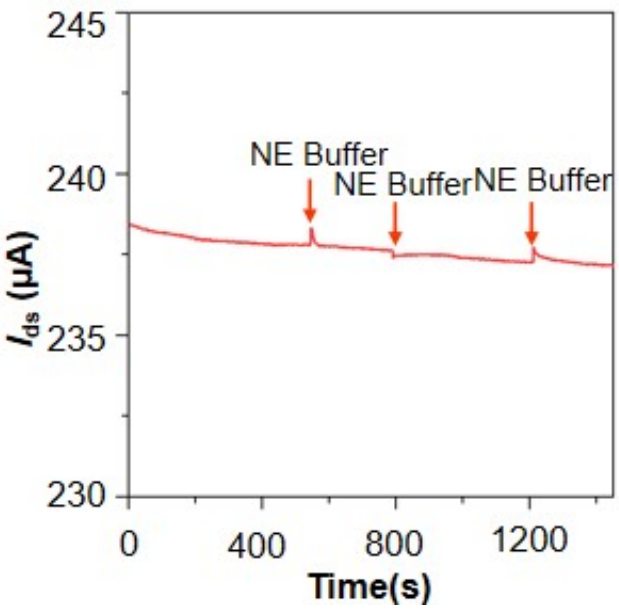

Fig. S9 I_{ds}-t curve of a Cas12a−GFET upon the addition of 1×NE buffer.

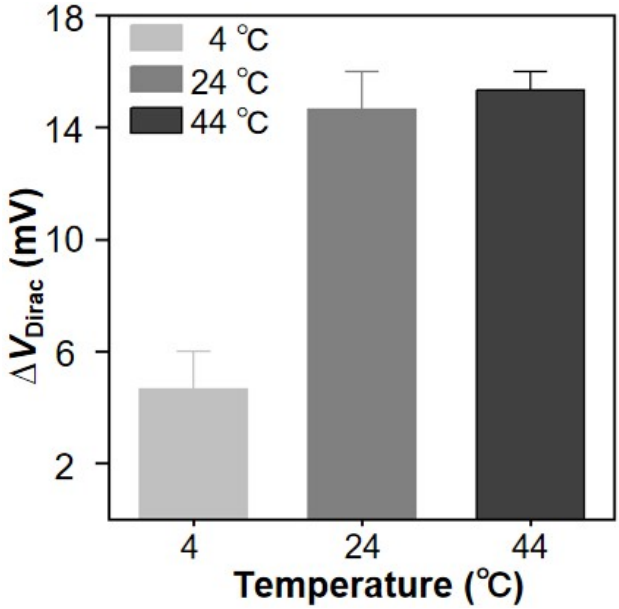

Fig. S10 $|\Delta V_{Dirac}|$ of Cas12a−GFET devices at different test temperatures upon the addition of Is1081 at concentrations of 6×10^{-16} M in 1×NE buffer.

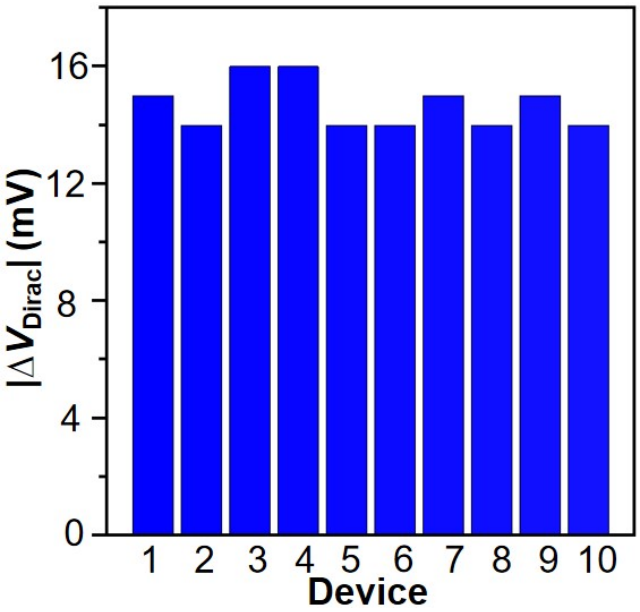

Fig. S11 $|\Delta V_{\mathrm{Dirac}}|$ of ten Cas12a–GFET devices upon the addition of Is1081 at concentrations of 6×10^{-16} M in 1×NE buffer.

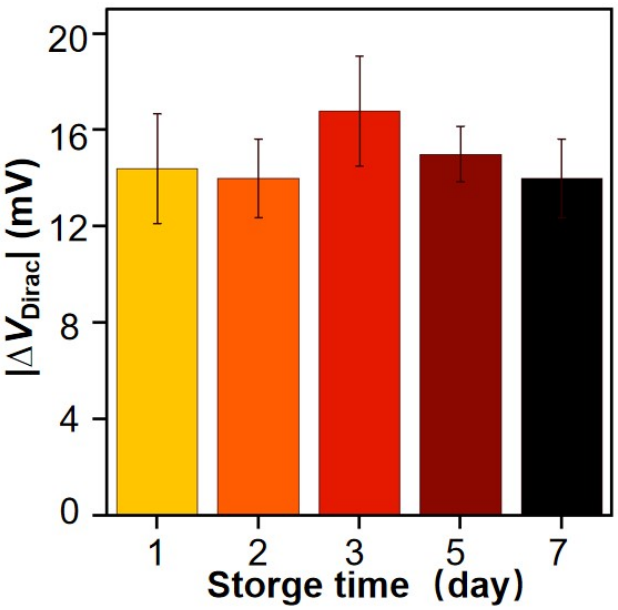

Fig. S12 After storage at room temperature for 1, 2, 3, 5, and 7 days, $|\Delta V_{\mathrm{Dirac}}|$ of Cas12a-GFET devices upon the addition of Is1081 at concentrations of 6×10^{-16} M in 1×NE buffer.

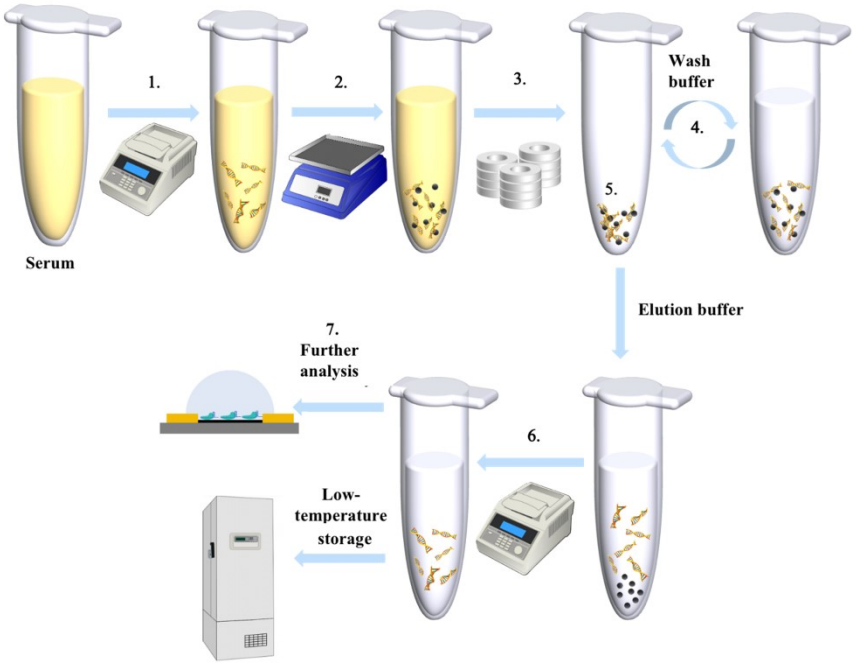

Figure S13. Magnetic beads method for nucleic acid extraction. The MagMAX™ DNA Multi-Sample Ultra 2.0 Kit is used to extract DNA from blood serum. The clinical serum samples are purified using magnetic beads following the procedures, namely, hydrolsis, binding, magnetic capture, washing, and elution. (1) Proteinase K is added to the samples. The mixture is vigorously vortexed and then incubated at 65 ℃ for 20 minutes. (2) After incubation, add DNA binding bead mixture and shake the samples at 800 rpm for 5 minutes. (3) The beads precipitate through the absorption of magnets for at least 5 minutes. The supernatant is carefully aspirated and all beads are collected. (4) Add 1mL wash solution I and shake at 800 rpm for 1 minute, magnetize the beads for 1 minute and discard the supernatant. Repeat with 1 mL wash solution II and 500 µL wash solution II. (5) Dry the beads by shaking at 900 rpm for 2 minutes. Add 100 µL elution solution and incubate at 70 ℃ for 5 minutes, shaking at 800 rpm for 5 minutes. (6) Magnetize for 3 minutes, discard the beads and carefully transfer the eluate. (7) Perform clinical testing or store in a freezer at −20 ℃.

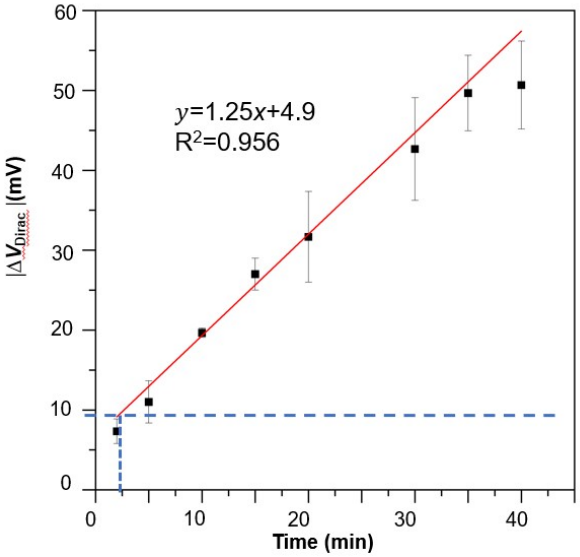

Figure S14. $|\Delta V_{\mathrm{Dirac}}|$ of Cas12a−GFETs measured within 40 minutes after the addition of clinical samples. The regression equation is calculated to be $y = 1.25x + 4.9$ with a correlation coefficient value (R^2) of 0.956. According to the cutoff value of 9.39 mV, the reaction time is calculated to be 3.6 minutes. Error bars are determined by the standard deviation from 3 devices.

Section S4 Supplementary tables

Table S1. The sequences (5'−3') of nucleotide chains used in this research.

DNA	Sequence
crRNA	UAAUUCUACUAAGUGUAGAUGUCAACCCAGCACCUGCCAG
Is1081	ATGACCTCTTCTCATCTTATCGACACCGAGCAGCTTCTGGCTGACC
	AACTCGCACAGGCGAGCCCGGATCTGCTGCGCGGGCTGCTCTCGA
	CGTTCATCGCCGCCTTGATGGGGGCTGAAGCCGACGCCCTGTGCGG
	GGCGGGCTACCGCGAACGCAGCGATGAGCGGTCCAATCAGCGCAA
	CGGCTACCGCCACCGTGATTTCGACACCCGTGCCGCAACCATCGAC
	GTCGCGATCCCCAAGCTGCGCCAGGGCAGCTATTTCCCGGACTGGC
	TGCTGCAGCGCCGCAAGCGAGCTGAACGCGCACTGACCAGCGTGG
	TGGCGACCTGCTACCTGCTGGGAGTATCCACTCGCCGGATGGAGCG
	CCTGGTCGAAACACTTGGTGTGACAAAGCTTTCCAAGTCGCAAGTG
	TCGATCATGGCCAAAGAGCTCGACGAAGCCGTAGAGGCGTTTCGG
	ACCCGCCCGCTCGATGCCGGCCCGTATACCTTCCTCGCCGCCGACG
	CCCTGGTGCTCAAGGTGCGCGAGGCAGGCCGCGTCGTCGGGGTGC
	ACACCTTGATCGCCACCGGCGTCAACGCCGAGGGCTACCGAGAGA
	TCCTGGGCATCCAGGTCACCTCCGCCGAGGACGGGGCCGGCTGGC
	TGGCGTTCTTCCGCGACCTGGTCGCCCGCGGCCTGTCCGGGGTCGC
	GCTGGTCACCAGCGACGCCCACGCCGGCCTGGTGGCCGCGATCGG
	CGCCACCCTGCCCGCAGCGGCCTGGCAGCGCTGCAGAACCCACTA
	CGCAGCCAATC
Escherichia coli	AGAGTTTGATCCTGGCTCAGATTGAACGCTGGCGGCAGGCCTAAC
gene for 16S	ACATGCAAGTCGAACGGTAACAGAAAGCAGCTTGCTGCTTTGCTG
rRNA	ACGAGTGGCGGACGGGTGAGTAATGTCTGGGAAACTGCCCGATGG
	AGGGGGATAACTACGGAAACGGTAGCTAATACCGCATAACGTCGC
	AAGACCAAAGAGGGGGACCTTGGGCCTCTTGCCATCGGATGTGCC
	CAGATGGGATTAGCTAGTAGGTGGGGTAAAGGCTCACCTAGGCGA
	CGATCCCTAGCTGGTCTGAGAGGATGACCAGCCACACTGGAACTG
	AGACACGGTCCAGACTCCTACGGGAGGCAGCAGTGGGGAATATTG
	CACAATGGGCGCAAGCCTGATGCAGCCATGCCGCGTGTATGAAGA
	AGGCCTTCGGGTTGTAAAGTACTTTCAGCGGGGAGGAAGGGAGTA
	AAGTTAATACCTTTGCTCATTGACGTTACCCGCAGAAGAAGCACCG
	GCTAACTCCGTGCCAGCAGCCGCGGTAATACGGAGGGTGCAAGCG
	TTAATCGGAATTACTGGGCGTAAAGCGCACGCAGGCGGTTTGTTAA
	GTCAGATGTGAAATCCCCGGGCTCAACCTGGGAACTGCATCTGATA
	CTGGCAAGCTTGAGTCTCGTAGAGGGGGGTAGAATTCCAGGTGTA
	GCGGTGAAATGCGTAGAGATCTGGAGGAATACCGGTGGCGAAGGC
	GGCCCCCTGGACGAAGACTGACGCTCAGGTGCGAAAGCGTGGGGA
	GCAAACAGGATTAGATACCCTGGTAGTCCACGCCGTAAACGATGT
	CGACTTGGAGGTTGTGCCCTTGAGGCGTGGCTTCCGGAGCTAACGC

	GTTAAGTCGACCGCCTGGGGAGTACGGCCGCAAGGTTAAAACTCA AATGAATTGACGGGGGCCCGCACAAGCGGTGGAGCATGTGGTTTA ATTCGATGCAACGCGAAGAACCTTACCTGGTCTTGACATCCACGGA AGTTTTCAGAGATGAGAATGTGCCTTCGGGAACCGTGAGACAGGT GCTGCATGGCTGTCGTCAGCTCGTGTTGTGAAATGTTGGGTTAAGT CCCGCAACGAGCGCAACCCTTATCCTTTGTTGCCAGCGGTCCGGCC GGGAACTCAAAGGAGACTGCCAGTGATAAACTGGAGGAAGGTGG GGATGACGTCAAGTCATCATGGCCCTTACGACCAGGGCTACACAC GTGCTACAATGGCGCATACAAAGAGAAGCGACCTCGCGAGAGCAA GCGGACCTCATAAAGTGCGTCGTAGTCCGGATTGGAGTCTGCAACT CGACTCCATGAAGTCGGAATCGCTAGTAATCGTGGATCAGAATGC CACGGTGAATACGTTCCCGGGCCTTGTACACACCGCCCGTCACACC ATGGGAGTGGGTTGCAAAAGAAGTAGGTAGCTTAACCTTCGGGAG GGCGCTTACCACTTTGTGATTCATGACTGGGGTGAAGTCGTAACAA GGTAACC
***Streptococcus agalactiae* Sip gene**	ATGGAAATGAATAAAAAGGTACTATTGACATCGACAATGGCAGCT TCGCTATTATCAGTCGCAAGTGTTCAAGCACAAGAAACAGATACG ACGTGGACAGCACGTACTGTTTCAGAGGTAAAGGCTGATTTGGTA AAGCAAGACAATAAATCATCATATACTGTGAAATATGGTGATACA CTAAGCGTTATTTCAGAAGCAATGTCAATTGATATGAATGTCTTAG CAAAAATTAATAACATTGCAGATATCAATCTTATTTATCCTGAGAC AACACTGACAGTAACTTACGATCAGAAGAGTCATACTGCCACTTCA ATGAAAATAGAAACACCAGCAACAAATGCTGCTGGTCAAACAACA GCTACTGTCGATTTGAAAACCAATCAAGTTTCTGTTGCAGACCAAA AAGTTTCTCTCAATACAATTTCGGAAGGTATGACACCAGAAGCAGC AACAACGATTGTTTCGCCAATGAAGACATATTCTTCTGCGCCAGCT TTGAAATCAAAAGAAGTATTAGCACAAGGGCAAGCTGTTAGTCAA GCAGCAGCTAATGAACAGGTATCACCAGCTCCTGTGAAGTCGATT ACTTCAGAAGTTCCAGCAGCTAAAGAGGAAGTTAAACCAACTCAG ACGTCAGTCAGTCAGTCAACAACAGTATCACCAGCTTCTGTTGCCG CTGAAACACCAGCTCCAGTAGCTAAAGTAGCACCGGTAAGAACTG TAGCAGCCCCTAGAGTGGCAAGTGTTAAAGTAGTCACTCCTAAAGT AGAAACTGGTGCATCACCAGAGCATGTATCAGCTCCAGCAGTTCCT GTGACTACGACTTCAACAGCTACAGACAGTAAGTTACAAGCGACT GAAGTTAAGAGCGTTCCGGTAGCACAAAAAGCTCCAACAGCAACA CCGGTAGCACAACCAGCTTCAACAACAAATGCAGTAGCTGCACAT CCTGAAAATGCAAGGCTCCAACCTCATGTTGCAGCTTATAAAGAA AAAGTAGCGTCAACTTATGGAGTTAATGAATTCAGTACATACCGTG CGGGAGATCCAGGTGATCATGGTAAAGGTTTAGCAGTTGACTTTAT TGTAGGTAAAAACCAAGCACTTGGTAACGAAGTTGCACAGTACTC TACACAAAATATGGCAGCAAATAACATTTCATATGTTATCTGGCAA CAAAAGTTTTACTCAAATACAAATAGTATTTATGGACCTGCTAATA CTTGGAATGCAATGCCAGATCGTGGTGGCGTTACTGCCAACCACTA TGACCACGTTCACGTATCCTTTAACTAA

Table S2. $|\Delta V_{Dirac}|$ of ten Cas12a−GFET devices upon the addition of Is1081.

Device number	$\lvert\Delta V_{Dirac}\rvert$ (mV)	C_1 (M)
1	15	4.77×10^{-16}
2	14	1.86×10^{-16}
3	16	1.22×10^{-15}
4	16	1.22×10^{-15}
5	14	1.86×10^{-16}
6	14	1.86×10^{-16}
7	15	4.77×10^{-16}
8	14	1.86×10^{-16}
9	15	4.77×10^{-16}
10	14	1.86×10^{-16}
Avergae	14.7	4.80×10^{-16}

Table S3. Results of clinical tests.

Sample number of TB patients	$\|\Delta V_{Dirac}\|$ **(mV)**	**Sample number of healthy people**	$\|\Delta V_{Dirac}\|$ **(mV)**
P1	48	N1	8
P2	38	N2	3
P3	40	N3	9
P4	29	N4	2
P5	23	N5	4
P6	28	N6	2
P7	24	N7	3
P8	49	N8	4
P9	26	N9	3
P10	25	N10	0
P11	25	N11	1
P12	30	N12	1
P13	26	N13	3
P14	27	N14	4
P15	21	N15	2
P16	24	N16	3
P17	27	N17	3
P18	30	N18	1
P19	41	N19	3
P20	18	N20	9
P21	19	N21	8
P22	13	N22	6
P23	15	N23	2
P24	31	N24	4
P25	40	N25	7
P26	25	N26	10
P27	27		
P28	29		
P29	50		
P30	21		

Table S4. Existing methods for TB detection and their performances.

Assay method	Detection probe	LoD	Specimen	Time(min)	Refs.
[a]LAMP	double-stranded DNA tail	4.3×10^{7} copies mL^{-1}	sputum	30	S6
CRISPR (an [b]MSPQC nucleic acid sensor based on CRISPR/Cas9)	single-stranded DNA	1.5×10^{4} copies mL^{-1}	sputum	120	S7
[c]IGRA	antibody	0.077 IU mL^{-1}	blood	15	S8
Piezoelectric assay (a sensor based on AuNPs-mediated enzyme)	hairpin DNA	1.5×10^{4} copies mL^{-1}	/	180	S9
Optical assay (POC)	antibody	1.6×10^{10} copies mL^{-1}	urine	15	S10
Magnetic assay ([d]MagPlas ELISA)	antibody	6.02×10^{6} copies mL^{-1}	urine	180	S11
Colorimetric assay (based on photo-polymerization)	DNA	3×10^{4} copies mL^{-1}	/	40	S12
		3×10^{5} copies mL^{-1}		90	
[e]NAAT	DNA	150 bacilli mL^{-1}	sputum	80	S13
Biophotonic assay	/	1.5×10^{6} RIU	blood	/	S14
Electrochemical assay	IS6110 sequence	6.77×10^{6} copies mL^{-1}	sputum	90	S15
		4.03×10^{6} copies mL^{-1}	culture	60	S16
		1.98×10^{8} copies mL^{-1}	serum	5	
	rpoB gene	2.4×10^{10} copies mL^{-1}	culture	30	

[a] Loop-mediated isothermal amplification; [b] Multi-channel series piezoelectric quartz crystal; [c] Interferon-gamma release assay; [d] Magnetoplasmonic; [e] Nucleic acid amplification testing.

References

1. Y. T. Chen, L. Sarangadharan, R. Sukesan, C. Y. Hseih, G. Y. Lee, J. I. Chyi and Y. L. Wang, *Sci. Rep.*, 2018, **8**, 8300.
2. A. Cao, M. Mescher, D. Bosma, J. H. Klootwijk, E. J. Sudholter and L. C. de Smet, *Anal. Chem.*, 2015, **87**, 1173−1179.
3. B. J. Kim, H. Jang, S. K. Lee, B. H. Hong, J. H. Ahn and J. H. Cho, *Nano Lett.*, 2010, **10**, 3464−3466.
4. C. Wang, Y. Li, Y. Zhu, X. Zhou, Q. Lin and M. He, *Adv. Funct. Mater*., 2016, ***26***, 7668−7678.
5. Q. Zhou, A. Rahimian, K. Son, D. S. Shin, T. Patel and A. Revzin, *Methods*., 2016, **97**, 88−93.
6. L. Liang, M. Chen, O. Hu, Q. He and Z. Chen, *Anal. Chem*., 2019, **91**, 6991–6995.
7. J. Huang, Z. Liang, Y. Liu, J. Zhou and F. He, *Anal. Chem.*, 2022, **94***,* 11409−11415.
8. J. J. Kim, Y. Park, D. Choi and H. S. Kim, *Ann. Lab. Med.*, 2020, **40**, 33−39.
9. J. Zhang and F. He, *Talanta.*, 2022, **236**, 122902.
10. P. Ramirez-Priego, D. Martens, A. A. Elamin, P. Soetaert, W. Van Roy, R. Vos, B. Anton, R. Bockstaele, H. Becker, M. Singh, P. Bienstman and L. M. Lechuga, *ACS Sens*., 2018, **3***,* 2079−2086.

11. J. Kim, V. T. Tran, S. Oh, M. Jang, D. K. Lee, J. C. Hong, T. J. Park, H. Kim and J. Lee, *ACS Cent. Sci.*, 2021*,* **7***,* 1898−1907.
12. E. Yee and S. H. Sike, *ACS Sens.*, 2020, ***5***, 308−312.
13. H. Krishna, N. Goyani Pratap and Mukhopadhyaya, *BioRixv*., 2023, 558062.
14. A. H. Aly, D. Mohamed, Z. A. Zaky, Z. S. Matar, N. S. Abd El-Gawaad, A. S. Shalaby, F. Tayeboun and M. Mohaseb, *Mater. Res.*, 2021, **24**, e20200483.
15. K. S. Rizi, B. Hatamluyi, M. Darroudi, Z. Meshkat, E. Aryan, S. Soleimanpour and M. Rezayi, *Microchem. J*., 2022, **179***,* 107467.
16. M. Chaturvedi, M. Patel, A. Tiwari, N. Dwivedi, D. P. Mondal, A. K. Srivastava and Dhand, C, *Mol. Biol*., 2023, **186**, 14−27.